**Research Article**

# Comparison between results of optical and electrical measurements of free electron concentration in *n*-InAs specimens

Tatyana G. Yugova[1], Aleksandr G. Belov[1], Vladimir E. Kanevskii[1], Evgeniya I. Kladova[1], Stanislav N. Knyazev[1], Irina B. Parfent'eva[1]

1  Federal State Research and Development Institute of Rare Metal Industry (Giredmet JSC), 2 Elektrodnaya Str., Moscow 111524, Russia

Corresponding author: Tatyana G. Yugova (P_Yugov@mail.ru)

**Citation:** Yugova TG, Belov AG, Kanevskii VE, Kladova EI, Knyasev SN, Parfent'eva IB (2021) Comparison between results of optical and electrical measurements of free electron concentration in *n*-InAs specimens. Modern Electronic Materials 7(3): 79–84. https://doi.org/10.3897/j.moem.7.3.76700

## Abstract

A theoretical model has been developed for determining the free electron concentration in *n*-InAs specimens from characteristic points in far IR reflection spectra. We show that this determination requires plasmon-phonon coupling be taken into account, otherwise the measured electron concentration proves to be overestimated. A correlation between the electron concentration $N_{opt}$ and the characteristic wavenumber $v_+$ has been calculated and proves to be well fit by a third order polynomial. The test specimens have been obtained by tin or sulfur doping of indium arsenide. The electron concentration in the specimens has been measured at room temperature using two methods: the optical method developed by the Authors ($N_{opt}$) and the conventional four-probe Hall method (the Van der Pau method, $N_{Hall}$). The reflecting surfaces of the specimens have been chemically polished or fine abrasive ground. The condition $N_{opt} > N_{Hall}$ has been shown to hold for all the test specimens. The difference between the optical and the Hall electron concentrations is greater for specimens having polished reflecting surfaces. The experimental data have been compared with earlier data for *n*-GaAs. A qualitative model explaining the experimental data has been suggested.

## Keywords

indium arsenide, electron concentration, Hall effect, reflection spectrum, plasmon-phonon coupling.

## 1. Introduction

The information value of experimental data increases greatly if the target parameter can be measured using different methods. It is recommendable to compare the different measurement data taking into account that each method has its specific features. For example the free carrier concentration in semiconductor specimens is typically measured using the Hall effect, either its classic six-probe variant or the more convenient four-probe Van der Pau modification.

Along with the Hall method the free carrier concentration in heavily doped semiconductors is often measured using the so-called plasma reflection method which is contactless and nondestructive unlike the Hall one. The spectral dependence of the reflection coefficient is recorded in the far IR region and the free carrier concentration is determined from the positions of the characteristic points.

It should be noted that free carrier concentration data obtained by electrical measurements represent the whole specimen bulk while those obtained by optical measurements only refer to the narrow superficial layer of the specimen. For this reason data obtained with these methods may differ. It was shown [1] that the free electron concentrations in n-GaAs calculated on the basis of Hall effect ($N_{Hall}$) may be either lower or higher than those determined from far IR reflection spectra ($N_{opt}$).

By analogy with the cited work [1] in which tellurium-doped gallium arsenide specimens were studied we present below the optical and electrical measurement data for sulfur- and tin-doped n-InAs specimens.

## 2. Experimental

The measurements were conducted for 21 n-InAs specimens 16 of which were sulfur-doped and 5 were tin-doped. The specimens were in the form of plane-parallel 6–10 mm side square wafers 1.03–2.26 mm in thickness (Table 1). ~2 mm thick wafers were cut from Cz-grown (100) single crystal indium arsenide ingots perpendicularly to the growth axis following which these wafers were cut into the specimens as described above. The specimens were then mechanically ground and chemically polished. The measurements were conducted at room temperature.

The contact material for electrical measurements was indium. Two specimens were placed on a holder one at each side and tinned copper contact wires were soldered to the holder outputs. The holder with the specimens was placed in the gap between electric magnet core poles perpendicularly to the magnetic field induction vector. The measurements were conducted at magnetic induction $B$ = 0.5 Tl and a 200 mA current passing through the specimen. Then the electrical resistivity $\rho$, the free electron concentration $N_{Hall}$ and the electron mobility $\mu$ were calculated. The relative random error of $N_{Hall}$ measurement was within ± 10 %.
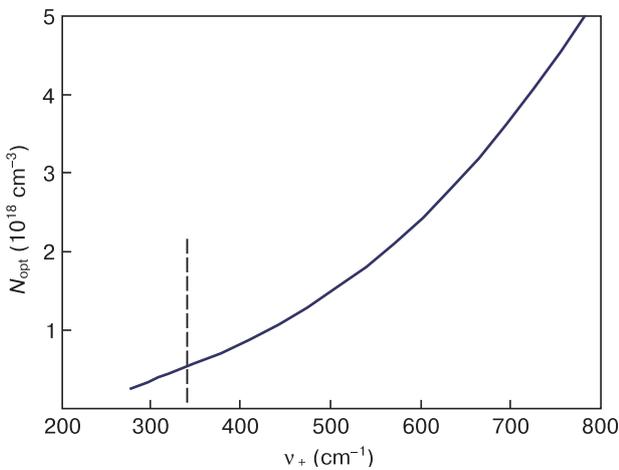


**Figure 1.** Calculated electron concentration *vs* characteristic wavenumber calibration curve. The vertical dotted line is the edge of the Tensor-27 Fourier spectrometer operation range

$N_{opt}$ was calculated from far IR reflection spectra (plasma resonance) [2–6] taking into account the interaction of plasma oscillations with longitudinal optical phonons (the plasmon-phonon coupling) [7–17]. The wavenumber dependence of the reflection spectrum $R(\nu)$ was recorded in the 340–1000 cm$^{-1}$ spectral range with a Tensor-27 Fourier spectrometer. Then the reflection spectra were processed using the Kramers–Kronig dispersion relations for the calculation of the real $\varepsilon_1(\nu)$ and imaginary $\varepsilon_2(\nu)$ parts of the complex dielectric permeability $\varepsilon = \varepsilon_1 + i\varepsilon_2$ and for the determination of the relationship between the imaginary part ($-1/\varepsilon$) and the wavenumber: $f_1(\nu) = Im(-1/\varepsilon) = \varepsilon_2/(\varepsilon_1^2 + \varepsilon_2^2)$ [18]. This relationship has a typical bell shape with a clear maximum [18–21]. Then the characteristic wavenumber $\nu_+$ corresponding to that maximum was determined and after that, based on the $\nu_+$ obtained, $N_{opt}$ was found using a calculated calibration curve.

More detailed information on $N_{opt}$ determination from the reflection spectrum was reported earlier for n-GaAs [1] and for n-InSb [22]. When plotting the $N_{opt} = f_2(\nu)$ calibration curve for n-InAs the non-parabolic shape of the conduction band of InAs was taken into account. Below are parameters included into the calculation formulae:

| | |
|---|---|
| Band gap $E_g$, eV | 0,36 [23] |
| HF dielectric permeability $\varepsilon_\infty$ | 11,6 [24] |
| Wavenumber at longitudinal optical phonon frequency $\nu_{LO}$, cm$^{-1}$ | 243 [24] |
| Wavenumber at transverse optical phonon frequency $\nu_{TO}$, cm$^{-1}$ | 219 [24] |
| Valence and conduction band interaction matrix element $P_{cv}$, eV · cm | 8.7 · 10$^{-8}$ [24] |

As a result the electron concentration *vs* characteristic wavenumber calibration curve was plotted (Fig. 1) which is described adequately well by a third order polynomial:

$$N_{opt} = 1.05 \cdot 10^{10}(\nu_+)^3 - 3.15 \cdot 10^{12}(\nu_+)^2 +$$
$$3.22 \cdot 10^{15}(\nu_+) - 6.27 \cdot 10^{17}. \tag{1}$$

Here $N_{opt}$ is in cm$^{-3}$ and $\nu_+$ is in cm$^{-1}$.

We show that the plasmon-phonon coupling being disregarded, $N_{opt}$ proves to be overestimated but this difference near the edge of the Tensor-27 Fourier spectrometer operation range is within 10% and decreases further with an increase in $\nu$. Note that the respective differences are 20% for n-GaAs [1] and 30% for n-InSb [22]. Since the absolute random error of $\nu_+$ is only controlled by spectral instrument resolution and is within ±2 cm$^{-1}$, the relative random error of $N_{opt}$ is within ±0.6 %.

## 3. Results and discussion

Table 1 shows the parameters of the test specimens, i.e., thickness (d), $\nu_+$, $N_{opt}$, $N_{Hall}$ (specimens are arranged

**Table 1.** Parameters of test specimens

| No. | Doping impurity | $d$ (mm) | $\nu_+$ (cm$^{-1}$) | $N_{opt}$ ($10^{18}$ cm$^{-3}$) | $N_{Hall}$ ($10^{18}$ cm$^{-3}$) | $\delta$ (%) |
|---|---|---|---|---|---|---|
| 1 | S | 1.30 | 369 | 0.660 | 0.564 | 14.5 |
| 2 | S | 1.50 | 457 | 1.19 | 1.04 | 12.6 |
| 3 | S | 1.74 | 491 | 1.43 | 1.28 | 10.5 |
| 4 | Sn | 1.03 | 496 | 1.48 | 1.27 | 14.2 |
| 5 | S | 2.26 | 532 | 1.78 | 1.59 | 10.7 |
| 6 | S | 1.90 | 538 | 1.83 | 1.59 | 13.1 |
| 7 | S | 1.77 | 545 | 1.89 | 1.79 | 5.3 |
| 8 | S | 1.93 | 573 | 2.15 | 1.93 | 10.2 |
| 9 | Sn | 1.43 | 591 | 2.34 | 2.14 | 8.5 |
| 10 | S | 1.39 | 600 | 2.43 | 1.95 | 19.8 |
| 11 | Sn | 1.24 | 617 | 2.63 | 2.32 | 11.8 |
| 12 | S | 1.01 | 635 | 2.84 | 2.44 | 14.1 |
| 13 | S | 1.57 | 639 | 2.89 | 2.50 | 13.5 |
| 14 | S | 2.12 | 656 | 3.09 | 2.79 | 9.7 |
| 15 | S | 1.47 | 668 | 3.25 | 2.95 | 9.2 |
| 16 | S | 1.75 | 673 | 3.31 | 3.11 | 6.0 |
| 17 | Sn | 1.10 | 677 | 3.36 | 2.98 | 11.3 |
| 18 | S | 2.17 | 678 | 3.38 | 3.05 | 9.8 |
| 19 | S | 1.79 | 683 | 3.44 | 3.09 | 10.2 |
| 20 | S | 1.92 | 684 | 3.46 | 3.13 | 9.5 |
| 21 | Sn | 1.32 | 684 | 3.46 | 2.92 | 15.6 |

*Note:* Reflection spectra for polished surfaces.

in order of increasing $N_{opt}$), as well as $\delta = 100\%(N_{opt} - N_{Hall})/N_{opt}$ characterizing the difference between the optical and Hall data.

As can be seen from Table 1 all the test specimens obey the relationship $N_{opt} > N_{Hall}$. The parameters $\delta$ is the highest for Specimen No. 10 (19.8%) and the lowest for Specimen No. 7 (5.3%).

Figure 2 shows the relationship between the Hall and optical electron concentrations which is described by the following linear function:

$$N_{Hall} = 0.9002 N_{opt} - 0.0309. \qquad (2)$$

When doing RMS linear approximation one should estimate the quality of the fit between the experimental points and the linear function. The criterion is the parameter $R^2$: the closer $R^2$ to unity the better the approximation. In the case considered $R^2 = 0.9896$ as calculated by the software along with the other approximation parameters.

It can be seen from Fig. 2 that both the sulfur- and the tin-doped specimens obey a similar regularity. The same is true for $\delta$ (Table 1).

One can therefore safely assure that there is a difference between $N_{Hall}$ and $N_{opt}$ and this difference is unilateral, i.e., $N_{Hall}$ anis always lower than $N_{opt}$. The random factor (scatter about a certain mean value) is also absent.

As noted above the result was different for $n$-GaAs: $N_{Hall}$ could be lower or higher than $N_{opt}$. The concentrations measured by the two methods were equal at

$N_{eq} = 1.07 \cdot 10^{18}$ cm$^{-3}$ [1]. For the low-doped material this ratio was < 1 but with an increase in the tellurium concentration the relation became > 1.

This difference in the behavior of doping impurities in GaAs and InAs single crystals can be accounted for by the difference in the homogeneity ranges of these compounds. Excess gallium or indium controls the bulk concentration of arsenic vacancies. As reported earlier [25] the homogeneity range of GaAs is substantially broader than that of InAs. In other words, the concentration of arsenic vacancies in InAs is much lower than in GaAs.
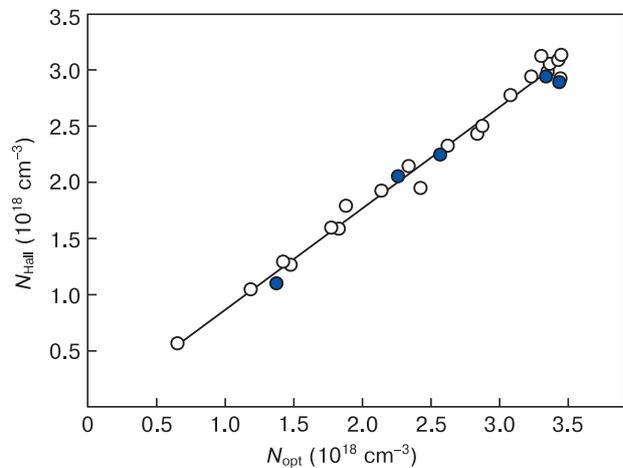


**Figure 2.** Hall *vs* optical electron concentration: white circle is sulfur-doped specimens and blue circle is tin-doped specimens.

**Table 2.** Optical and electrical measurement data on electron concentration for polished and ground reflecting surfaces of specimens

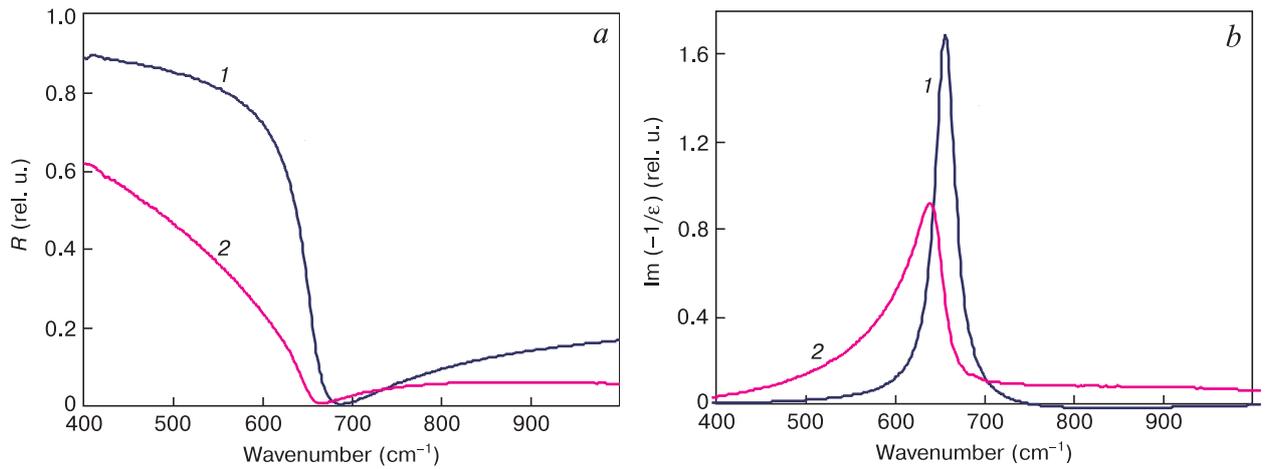| No. | Reflecting surface treatment | $d$ (mm) | $\nu_+$ (cm$^{-1}$) | $N_{opt}$ ($10^{18}$ cm$^{-3}$) | $N_{Hall}$ ($10^{18}$ cm$^{-3}$) | $\Delta N$ ($10^{17}$ cm$^{-3}$) |
|---|---|---|---|---|---|---|
| 1 | Polished | 1.30 | 369 | 6.60 | 5.64 | 0.96 |
|   | Ground   | 1.14 | 364 | 6.35 | 5.67 | 0.68 |
| 10 | Polished | 1.39 | 600 | 2.43 | 1.95 | 4.8 |
|    | Ground   | 1.42 | 597 | 2.40 | 2.21 | 1.9 |
| 14 | Polished | 2.12 | 656 | 3.09 | 2.79 | 3.0 |
|    | Ground   | 2.05 | 639 | 2.89 | 2.69 | 2.0 |
| 18 | Polished | 2.17 | 678 | 3.38 | 3.05 | 3.3 |
|    | Ground   | 2.00 | 667 | 3.24 | 3.05 | 1.9 |

*Note:* $\Delta N = N_{opt} - N_{Hall}$.



**Figure 3.** (*a*) reflection spectra of Specimen No. 14 for the polished surface (Curve *1*) and the ground surface (Curve *2*) and (*b*) $f_1(\nu) = \mathrm{Im}(-1/\varepsilon)$ functions for reflection spectra of Curves *1* and *2* of the same specimen

The lower arsenic vacancy concentration determines the smaller fraction of the electrically neutral doping impurity in the bulk which forms complexes with arsenic vacancies. During Hall measurements the magnetic field destroys these complexes to transfer the impurity to an electrically active state thus increasing the $N_{Hall}$ concentration [21]. However since the fraction of the electrically neutral doping impurity is but low, the $N_{Hall}$ concentration unlike that for tellurium-doped GaAs crystals cannot become higher than the $N_{opt}$ concentration which is confirmed by the experiment. Furthermore the arsenic vacancy concentration on the wafer surface is very low and as a result almost all the doping impurity is in an electrically active state thus ensuring the highest $N_{opt}$ concentration.

As we showed earlier [1] the $N_{Hall}/N_{opt}$ *vs* $N_{Hall}$ dependence for GaAs is described by a parabolic function and this ratio tends to unity with an increase in $N_{Hall}$. Unfortunately InAs exhibits a significant scatter of experimental points and therefore one cannot trace any regularity. However the tendency of decreasing the difference between the optical and Hall measurement data with an increase in $N_{Hall}$ persists.

It is a well-known practice for optical measurements to thoroughly polish the reflecting surface of the test specimen to a mirror-like condition. The question arises, what if the quality of the reflecting surface is intentionally degraded, i.e., the specimen is abrasive ground so the reflecting surface becomes matted? How strongly will the optical properties of the specimen and hence $N_{opt}$ change?

With this task in mind, we conducted the following experiment: we ground the reflecting surfaces of four specimens out of those listed in Table 1 with M10 grinding powder (grain size 10 μm) so they became matted. Then we recorded reflection spectra and calculated $N_{opt}$ following which we repeated electrical measurements.

Figure 3 *a* shows the reflection spectra of Specimen No. 14 (Table 1) for the polished surface (Curve *1*) and for the ground surface (Curve *2*). Figure 3 *b* shows the $f_1(\nu) = \mathrm{Im}(-1/\varepsilon)$ functions for the reflection spectra of Curves *1* and *2* of the same specimen in the same scale.

As can be seen from Fig. 3 *a* degradation of the reflectivity of the specimen surface causes a shift of the reflection spectrum towards lower wavenumbers indicating a decrease in $N_{opt}$, smearing of the leading edge of the $R(\nu)$ curve and a decrease in the absolute values of the reflection coefficient. Therefore the $f_1(\nu) = \mathrm{Im}(-1/\varepsilon)$ function is also smeared and its maximum also shifts towards lower $\nu$. When recalculated to $N_{opt}$, the decrease proves to be but minor (Table 2).

Table 2 shows optical and electrical measurement data for four specimens out of those listed in Table 1 (the original specimen numbers are kept).

It can be seen from Table 2 that $\nu_+$ of polished surface is greater than that of ground surface, indicating a decrease in $N_{opt}$ for lower surface quality. $\Delta N$ decreases also, i.e., the optical data for ground surface are in a better agreement with the Hall data.

Furthermore the $N_{opt}$ concentration in all the test specimens decreases after surface grinding and becomes closer to the $N_{Hall}$ concentration (Table 2). The origin of this change in the $N_{opt}$ concentration is not quite clear but one can assume that grinding of specimen surface uncovers the crystal bulk where the vacancy concentration is higher than at the wafer surface and the doping impurity forms complexes with arsenic vacancies. These complexes reduce the fraction of the electrically active doping impurity in the crystal bulk and hence lead to a decrease in $N_{opt}$. However $N_{opt}$ anyway remains higher than $N_{Hall}$ which is not quite clear either.

Thus one can assert that there is a systematic difference between the $N_{opt}$ and $N_{Hall}$ concentrations, the former concentration always being higher. This difference is smaller for ground specimen surface.

Note that this study was undertaken in order to explore the possibility of transition from the conventional Hall method of free electron concentration measurement to a more convenient optical one. The experimental results reported in this work should be taken into account.

# 4. Conclusion

A theoretical model was developed for determining the free electron concentration in $n$-InAs specimens ($N_{opt}$) from characteristic points in far IR reflection spectra. We showed that $N_{opt}$ determination requires plasmon-phonon coupling be taken into account, otherwise the measured $N_{opt}$ electron concentration proves to be 10% overestimated. A correlation between the electron concentration and the characteristic wavenumber was calculated and proves to be well fit by a third order polynomial.

The free electron concentration in the specimens was measured using two methods: based on reflection spectra ($N_{opt}$) and using the conventional Van der Pau method ($N_{Hall}$), for different treatment of specimen reflection surface: chemical polishing and fine abrasive grinding. The condition $N_{opt} > N_{Hall}$ was shown to hold for all the test specimens. The difference between the optical and the Hall electron concentrations proved to be greater for specimens having polished reflecting surfaces.

The experimental data were compared with earlier data for $n$-GaAs. A qualitative model explaining the experimental data was suggested.

# References

1. Yugova T.G., Belov A.G., Kanevskii V.E., Kladova E.I., Knyazev S.N. Comparison between optical and electrophysical data on free electron concentration in tellurim doped $n$-GaAs. *Modern Electronic Materials*, 2020; 6(3): 85–89. https://doi.org/10.3897/j.moem.6.3.64492

2. Galkin G.N., Blinov L.M., Vavilov V.S., Solomatin A.G. Plasma resonance on nonequilibrium carriers in semiconductors. *Pis'ma v zhurnal tekhnicheskoi fiziki*, 1968; 7(3): 93–96. (In Russ.)

3. Belogorokhov A.I., Belov A.G., Petrovitch P.L., Rashevskaya E.P. Determination of the concentration of free charge carriers in $Pb_{1-x}Sn_xTe$ taking into account the damping of plasma oscillations. *Optika i spektroskopiya*, 1987; 63(6): 1293–1296. (In Russ.)

4. Belogorokhov A.I., Belogorokhova L.I., Belov A.G., Rashevskaya E.P. Plasma resonance of free charge carriers and estimation of some parameters of the band structure of the material $Cd_xHg_{1-x}Te$. *Fizika i tekhnika poluprovodnikov*, 1991; 25(7): 1196–1203. (In Russ.). URL: https://journals.ioffe.ru/articles/viewPDF/23491

5. Sharov M.K. Plasma resonance in $Pb_{1-x}Ag_xTe$ alloys. *Semiconductors*, 2014; 48(3): 299–301. https://doi.org/10.1134/S1063782614030245

6. Rokakh A.G., Shishkin M.I., Skaptsov A.A., Puzynya V.A. On the possibility of the plasma resonance in CdS–PbS films in the middle infrared region. *Prikladnaya Fizika*. 2014; (5): 58–60. (In Russ.)

7. Varga B.B. Coupling of plasmons to polar phonons in degenerate semiconductors. *Phys. Rev.,* 1965; 137(6A): 1896–1901. https://doi.org/10.1103/PhysRev.137.A1896

8. Singwi K.S., Tosi M.P. Interaction of plasmons and optical phonons in degenerate semiconductors. *Phys. Rev.*, 1966; 147(2): 658–662. https://doi.org/10.1103/PhysRev.147.658

9. Shkerdin G., Rabbaa S., Stiens J., Vounckx R. Influence of electron scattering on phonon-plasmon coupled modes dispersion and free electron absorption in $n$-doped GaN semiconductors at mid-IR wavelengths. *Phys. Status Solidi (b)*, 2014; 251(4): 882–891. https://doi.org/10.1002/pssb.201350039

10. Ishioka K., Brixius K., Höfer U., Rustagi A., Thatcher E.M., Stanton C.J., Petek Hr. Dynamically coupled plasmon-phonon modes in GaP: an indirect-gap polar semiconductor. *Phys. Rev. B*. 2015; 92(20): 205203. https://doi.org/10.1103/PhysRevB.92.205203

11. Volodin V.A., Efremov M.D., Preobrazhensky V.V., Semyagin B.R., Bolotov V.V., Sachkov V.A., Galaktionov E.A., Kretinin A.V. Investigation of phonon-plasmon interaction in GaAs/AlAs tunnel superlattices. *Pis'ma v zhurnal tekhnicheskoi fiziki*. 2000; 71(11): 698–704. (In Russ.)

12. Kulik L.V., Kukushkin I.V., Kirpichev V.E., Klitzing K.V., Eberl K. Interaction between intersubband Bernstein modes and coupled plasmon-phonon modes. *Phys. Rev, B*, 2000; 61(19): 12717–12720. https://doi.org/10.1103/PhysRevB.61.12717

13. Mandal P.K., Chikan V. Plasmon-phonon coupling in charged $n$-type CdSe quantum dots: a THz time-domain spectroscopic study. *Nano Lett.*, 2007; 7(8): 2521–2528. https://doi.org/10.1021/nl070853q

14. Stepanov N., Grabov V. Optical properties of $Bi_{1-x}Sb_x$ crystals, related electron-plasmon and plasmon-phonon interactions. *Izv. RGPU im. Gertsena*, 2004; 4(8): 52–64. (In Russ.)

15. Trajic J., Romcevic N., Romcevic M., Nikiforov V.N. Plasmon-phonon and plasmon-two different phonon interaction in $Pb_{1-x}Mn_xTe$ mixed crystals. *Mater. Res. Bull.*, 2007; 42(12): 2192–2201. https://doi.org/10.1016/j.materresbull.2007.01.003

16. Chudzinski P. Resonant plasmon-phonon coupling and its role in magneto-thermoelectricity in bismuth. *Eur. Phys. J. B*, 2015; 88(12): 344. https://doi.org/10.1140/epjb/e2015-60674-3

17. Belov A.G., Denisov I.A., Kanevskii V.E., Pashkova N.V., Lysenko A.P. Determining the free carrier density in $Cd_xHg_{1-x}Te$ solid solutions from far-infrared reflection spectra. *Semiconductors*, 2017; 51(13): 1732–1736. https://doi.org/10.1134/S1063782617130048

18. Yu P. Y., Cardona M. Fundamentals of Semiconductors. Berlin; Heidelberg: Springer-Verlag 2010, 778 p. https://doi.org/10.1007/978-3-642-00710-1

19. Vinogradov E.A., Vodopyanov L.K. Graphical method for determining phonon frequencies from reflection spectra of crystals in the far infrared region of the spectrum. *Kratkie soobtsheniya po fizike*, 1972; (11): 29–32. (In Russ.)

20. Belogorokhov A.I., Belogorokhova L. I. Optical phonons in cylindrical filaments of porous GaP. *Fizika tverdogo tela*, 2001; 43(9): 1693–1697. (In Russ.). URL: https://journals.ioffe.ru/articles/viewPDF/38320

21. Yugova T.G., Belov A.G., Knyazev S.N. Magnetoplastic effect in Te-doped GaAs single crystals. Crystallography Reports, 2020; 65(1); 7–11. https://doi.org/10.1134/S1063774520010277

22. Belova I.M., Belov A.G., Kanevskii V.E., Lysenko A.P. Determining the concentration of free electrons in *n*-InSb from far-infrared reflectance spectra with allowance for plasmon-phonon coupling. *Semiconductors*, 2018; 52(15): 1942–1946. https://doi.org/10.1134/S1063782618150034

23. Pankove J.I. *Optical processes in semiconductors*. New York: Prentice Hall, 1971, 422 p.

24. Madelung O. Physics of III-V compounds. New York: John Wiley & Sons, Inc., 1964, 409 p.

25. Bublik V.T., Milvidsky M.G. Intrinsic point defects, nonstoichiometry and microdefects in $A^3B^5$ compounds. *Materialovedenie*, 1997; (2): 21–29. (In Russ.)